Effects of boundary on momentum distribution of quarks in a quark-gluon plasma

Cheuk-Yin Wong
Oak Ridge National Laboratory, Oak Ridge, Tennessee 37831
(Received 9 September 1992)

The boundary of a quark-gluon plasma affects the momentum distribution of quarks and consequently the magnitudes of signals for the search of the quark-gluon plasma.

PACS number(s): 24.85.+p, 12.38.Mh, 25.75.+r

Recently, there has been much interest in the possible existence of the quark-gluon plasma [1]. It is expected that under high temperature or high baryon density, quarks and gluons are deconfined to become a quark-gluon plasma. The deconfinement refers to the circumstances where a quark or an antiquark is not confined within the spatial dimension of a hadron. Quarks are nonetheless confined within the boundary of the plasma. Under laboratory conditions where a quark-gluon plasma may be produced by using relativistic heavy-ion collisions, the expected initial transverse radius of the quark-gluon plasma is of the order of the radius of the smaller of the two colliding nuclei producing the plasma, a dimension of a few fermis. Therefore, a necessary and sufficient condition for the existence of a quark-gluon plasma in heavy-ion reactions is that the quarks in the plasma can travel freely within a spatial region of many fermis. The distribution of the transverse momenta provides information on the transverse boundary for the motion of the quarks. It can be used to detect the presence of a quark-gluon plasma. Furthermore, the magnitudes of the signals for quark-gluon plasma detection are functions of the momentum distribution of the quarks, which has been generally taken to be that of a thermal distribution [2–4]. As the presence of the boundary affects the momentum distribution, the boundary effects must be taken into account in order to give a better estimate of the magnitudes of signals to search for the plasma.

The boundary effects are of interests also to other branches of physics. As a problem in general quantum mechanics, one wishes to know how the momentum distribution of a fermion system changes as the boundary extends to greater and greater distances, and what part of the distribution shows the effects of boundary and what part is well described by the Fermi-Dirac distribution. The effects arise because the existence of the boundary leads to the vanishing of the wave functions at the exterior regions. The decrease of the wave functions from the interior region to the exterior region gives rise to the presence of an enhanced high-momentum component relative to the Fermi-Dirac distribution. The boundary also leads to oscillations of the momentum distribution in the low-momentum region due to the uncertainty principle and the nonuniformity of single-particle energies. We wish to study here the effects of the boundary on the momentum distribution of quarks in the quark-gluon plasma, using wave functions which satisfy the boundary conditions.

Previously, Elze and Greiner [5] studied the size effects on the momentum distribution of a spherical plasma droplet. Unfortunately, in their expression for the momentum distribution [Eq. (20) of Ref. 5], the momentum wave functions of the single-particle states are incorrectly missing. For a finite system, the momentum distribution depends crucially on the momentum wave functions. Without the momentum wave functions, Elze and Greiner could not study effects which are associated with the wave functions, such as the boundary effects discussed here.

We consider a quark-gluon plasma in a cylinder of radius r_0 and length L, which is presumably formed after a relativistic nucleus-nucleus collision. We study the motion of a quark or an antiquark confined in this region, with the transverse potential represented by a scalar potential $m(r)$. The Dirac equation for the quark in cylindrical coordinates (r,ϕ,z) is

$$\left[\gamma^\mu \cdot p_\mu - m(r)\right]\psi(r,\phi,z) = 0.$$

Separation of variables is possible if one assumes a wave function of the form [6–9]

$$\psi(r,\phi,z) = \begin{pmatrix} R_{1\nu}(r)e^{i\nu\phi}\Phi_1(z) \\ -iR_{2\nu}(r)e^{i(\nu+1)\phi}\Phi_2(z) \\ R_{1\nu}(r)e^{i\nu\phi}\Phi_2(z) \\ iR_{2\nu}(r)e^{i(\nu+1)\phi}\Phi_1(z) \end{pmatrix}.$$

The equations for $\Phi_1(z)$ and $\Phi_2(z)$ are

$$\left(E^2 + \partial_z^2 - m^{*2}\right)\Phi_i(z) = 0, \tag{1}$$

with the solution

$$\Phi_1(z) = f_{n\lambda}(z)$$
$$= \sqrt{\frac{1}{L}}\delta_{n0} + (1-\delta_{n0})\sqrt{\frac{2}{L}}\sin[\Pi_{n\lambda}z + (1+\lambda)\pi/4]$$

and

$$\Phi_2(z) = -i\frac{1}{E+m^*}\partial_z\Phi_1(z),$$

where $\lambda = \pm 1$ and $\{\Pi_{n\lambda}\}$ are the eigenvalues determined by the bag boundary condition $i\Phi_1(\pm L/2) = \Phi_2(\pm L/2)$. The equations which couple $R_{1\nu}$ and $R_{2\nu}$ are

 ©1993 The American Physical Society

$$\frac{\partial^2}{\partial r^2}R_{1\nu}(r)+\frac{1}{r}\frac{\partial}{\partial r}R_{1\nu}(r)-\frac{\nu^2}{r^2}R_{1\nu}(r)$$

$$+[m^{*2}-m^2(r)]R_{1\nu}(r)=-R_{2\nu}(r)\frac{\partial}{\partial r}m(r), \quad (2a)$$

$$\frac{\partial^2}{\partial r^2}R_{2\nu}(r)+\frac{1}{r}\frac{\partial}{\partial r}R_{2\nu}(r)-\frac{(\nu+1)^2}{r^2}R_{2\nu}(r)$$

$$+[m^{*2}-m^2(r)]R_{2\nu}(r)=-R_{1\nu}(r)\frac{\partial}{\partial r}m(r), \quad (2b)$$

where $\{m^*\}$ are the eigenvalues for states satisfying the boundary conditions that $R_{i\nu}(r)\to 0$, as $r\to\infty$, and $E^2=\Pi_{n\lambda}^2+m^{*2}$.

We introduce the Fourier transform of $f_{n,\lambda}(z)$ and $R_{i\nu}$ by

$$\mathcal{F}_{n\lambda}(p_z)=\frac{1}{\sqrt{2\pi}}\int dz\, e^{ip_z z}f_{n\lambda}(z) \quad (3)$$

and

$$\mathcal{R}_{i\nu}(p_T)e^{i\nu\phi_p}=\frac{1}{2\pi}\int d\mathbf{r}\, e^{i\mathbf{p}_T\cdot\mathbf{r}}R_{i\nu}(r)e^{i\nu\phi}. \quad (4)$$

Then, the wave function ψ for the state $(n\lambda\nu)$ in momentum space is

$$\psi_{n\lambda\nu}(\mathbf{p})=\begin{pmatrix}\mathcal{R}_{1\nu}(p_T)e^{i\nu\phi_p}\\ -i\mathcal{R}_{2\nu}(p_T)e^{i(\nu+1)\phi_p}p_z/(E+m^*)\\ \mathcal{R}_{1\nu}(p_T)e^{i\nu\phi_p}p_z/(E+m^*)\\ i\mathcal{R}_{2\nu}(p_T)e^{i(\nu+1)\phi_p}\end{pmatrix}\mathcal{F}_{n\lambda}(p_z).$$

The momentum density $j^0_{n\lambda\nu}(\mathbf{p})$ for a quark in the state $n\lambda\nu$ is given by

$$j^0_{n\lambda\nu}(\mathbf{p})=\overline{\psi_{n\lambda\nu}(\mathbf{p})}\,\gamma^0\psi_{n\lambda\nu}(\mathbf{p})$$
$$=[|\mathcal{R}_{1\nu}(p_T)|^2+|\mathcal{R}_{2\nu}(p_T)|^2]\times\left(1+\frac{p_z^2}{(E+m^*)^2}\right)|\mathcal{F}_{n\lambda}(p_z)|^2.$$

For a given set of quantum numbers $(n\lambda\nu)$, there can be many different transverse eigenstates. Each state is characterized by additional quantum numbers $s\pm$. In a quark-gluon plasma at a temperature T with a chemical potential μ, the momentum distribution of the quarks is given by

$$\frac{dN_q}{d^3p}=g_q\sum_{n,\lambda,\nu,s\pm}[1+\exp\{(E_{n\lambda\nu s\pm}-\mu)/T\}]^{-1}\times[|\mathcal{R}_{1\nu,s\pm}(p_T)|^2+|\mathcal{R}_{2\nu,s\pm}(p_T)|^2]\times\left(1+\frac{p_z^2}{(E_{n\lambda\nu s\pm}+m^*_{\nu s\pm})^2}\right)|\mathcal{F}_{n,\lambda}(p_z)|^2, \quad (5)$$

where the degeneracy g_q is the product of the number of colors N_c, the number of flavors N_f, and the number of spins N_s.

To get a general idea of the boundary effects, we consider the case $L\to\infty$, $p_z=0$ and a sharp boundary with $m(r)=m_0$ for $r\le r_0$ and $m(r)\to\infty$ for $r>r_0$. The radial wave functions are [6–9]

$$R_{1\nu}(r)=AJ_{\nu+1}(Cr_0)J_\nu(Cr),$$

$$R_{2\nu}(r)=AJ_\nu(Cr_0)J_{\nu+1}(Cr),$$

where J_ν are the Bessel functions of the first kind of order ν and A is a normalization constant. The quantity C is obtained by solving the eigenvalue equation

$$J_{\nu\pm1}(x_\pm)=\pm f(x_\pm)J_\nu(x_\pm), \quad (6)$$

where $x=Cr_0$ and

$$f(x_\pm)=\frac{\sqrt{x^2+(m_0r_0)^2}\pm m_0r_0}{x}. \quad (7)$$

For a given value of ν, the solution of this equation leads to a discrete set of allowed values for C characterized by additional quantum numbers $(s\pm)$, where s corresponds to the sth solution of Eqs. (6) and (7), and the $\pm$ sign corresponds to the two different signs of Eq. (6).

The Fourier transform of the Bessel function is

$$\mathcal{J}_{\nu,s\pm}(p_Tr)=\frac{1}{2\pi}\int_0^{r_0}dr\,r\int_0^{2\pi}d\phi\,e^{-ip_Tr\sin\phi}\times e^{i\nu\phi}J_\nu(C_{\nu,s\pm}r),$$

which gives [10]

$$\mathcal{J}_{\nu,s\pm}\,(p_Tr_0)=\frac{r_0}{p_T^2-C_{\nu,s\pm}^2}\left[-C_{\nu,s\pm}\,J_\nu(p_Tr_0)\,J_{\nu+1}(C_{\nu,s\pm}r_0)+p_T\,J_{\nu+1}(p_Tr_0)\,J_\nu(C_{\nu,s\pm}r_0)\right]. \quad (8)$$

For $p_T\gg 1/r_0$, the function $\mathcal{J}_{\nu,s\pm}$ varies as p_T^{-3}.

The distribution of the transverse momenta of quarks at a temperature T and a chemical potential μ, at $p_z=0$, is therefore

$$\frac{dN_q}{d^3p(dz/2\pi)}=g_q\sum_{\nu,s\pm}\left(1+\exp\{(E_{\nu s\pm}-\mu)/T\}\right)^{-1}\times\mathcal{N}^{-1}_{\nu,s\pm}\left\{|J_{\nu+1,s\pm}(C_{\nu,s\pm}r_0)|^2|\mathcal{J}_{\nu,s\pm}(p_Tr_0)|^2+|J_{\nu,s\pm}(C_{\nu,s\pm}r_0)|^2|\mathcal{J}_{\nu+1,s\pm}(p_Tr_0)|^2\right\}, \quad (9)$$

where

$$\mathcal{N}_{\nu,s\pm}=\int_0^\infty 2\pi dp_T p_T\left\{|J_{\nu+1,s\pm}(C_{\nu,s\pm}r_0)|^2|\mathcal{J}_{\nu,s\pm}(p_Tr_0)|^2+|J_{\nu,s\pm}(C_{\nu,s\pm}r_0)|^2|\mathcal{J}_{\nu+1,s\pm}(p_Tr_0)|^2\right\}. \quad (10)$$

If the quark-gluon plasma is in a continuum without a boundary, the transverse momentum distribution for massless quarks with $\mu = 0$ and $p_z = 0$ will be given by the Fermi-Dirac distribution $dN_q/d^3p(dz/2\pi) = [g_q\pi r_0^2/(2\pi)^2]/[1+e^{-p_T/T}]$ (the dashed curves in Fig. 1). The solid curves in Fig. 1 give the distributions of the transverse momenta of quarks for $r_0 = 2$, 4, and 6 fm at $T = 200$ MeV obtained by using Eqs. (9) and (10). The momentum distribution for $r_0 = 2$ fm is quite different from a Fermi-Dirac distribution. As the radius increases to 4 fm and larger, the momentum distribution is quite close to the Fermi-Dirac distribution over a large range of momentum. However, in the regions of very small and very large momenta, there are significant qualitative differences. In the region of small transverse momenta with $p_T \sim \hbar/r_0$, there is a small peak due to the uncertainty principle and the nonuniformity of single-particle energies, and the magnitude of the distribution is slightly less than the Fermi-Dirac distribution. As the radius increases, the small momentum peak becomes sharper and sharper. On the other hand, in the high-transverse-momentum region, there is a high-momentum tail, which varies with the transverse momentum by a power law and is greater than the Fermi-Dirac distribution by orders of magnitude. The location at which the distribution begins to differ substantially from the Fermi-Dirac distribution increases with the radius of the system.

How do the magnitudes of the signals estimated by using momentum distribution for a system with a finite transverse boundary differ from the magnitudes estimated earlier [2–4] by using the Fermi-Dirac distribution? It is easy to generalize the results of Ref. [3] to a quark distribution of the general form $dN_q/d^3pd^3x = [g_q/(2\pi)^3]f(E)$, and show that the distribution for the invariant mass M of a dilepton pair produced by the quarks and the antiquarks of the plasma is given by

$$\frac{dN_{l^+l^-}}{dM^2d^4x} = g_qN_s\frac{\sigma(M)}{2(2\pi)^4}M^2\left(1-\frac{4m_a^2}{M^2}\right)^{\frac{1}{2}}f(\epsilon)F(M^2/4\epsilon)\sqrt{\frac{2\pi}{w(\epsilon)}}, \tag{11}$$

and the distribution in dilepton transverse mass $M_T = \sqrt{M^2+P_T^2}$ is

$$\frac{dN_{l^+l^-}}{dM^2dM_T^2d^4x} = g_qN_s\frac{\sigma(M)}{2(2\pi)^4}M^2\left(1-\frac{4m_a^2}{M^2}\right)^{\frac{1}{2}}\left\{-\frac{d}{dM_T^2}\left(\left[f(\epsilon)F(M_T^2/4\epsilon)\sqrt{\frac{2\pi}{w(\epsilon)}}\right]_{\epsilon=\epsilon(M_T)}\right)\right\}, \tag{12}$$

where $\sigma(M)$ is the $q\bar{q} \to l^+l^-$ cross section, m_a is the mass of the quark, $F(E) = -\int^E f(E')dE'$, $\epsilon(M)$ is the root of the equation

$$\left\{\frac{d}{dE}\left[\ln f(E) + \ln F\left(\frac{M^2}{4E}\right)\right]\right\}_{E=\epsilon} = 0, \tag{13}$$

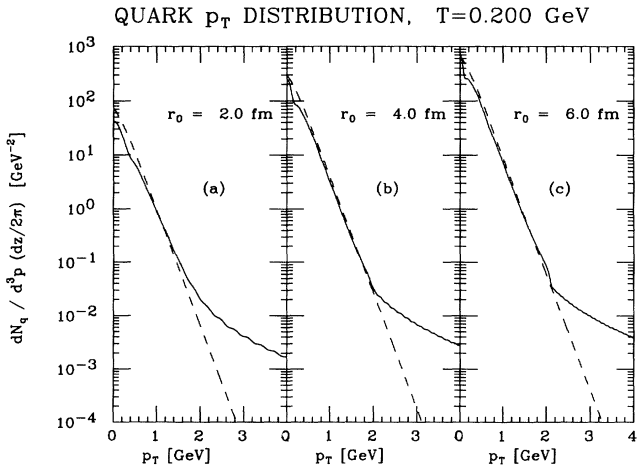

FIG. 1. Distribution of transverse momentum p_T of quarks in cylinders of different transverse radii. The radius is 2 fm in (a), 4 fm in (b), and 6 fm in (c). The temperature is taken to be 200 MeV and $p_z = 0$. Solid curves are the numerical results for a quark-gluon plasma with the boundary, and the dashed curves are the predictions from the Fermi-Dirac distribution.

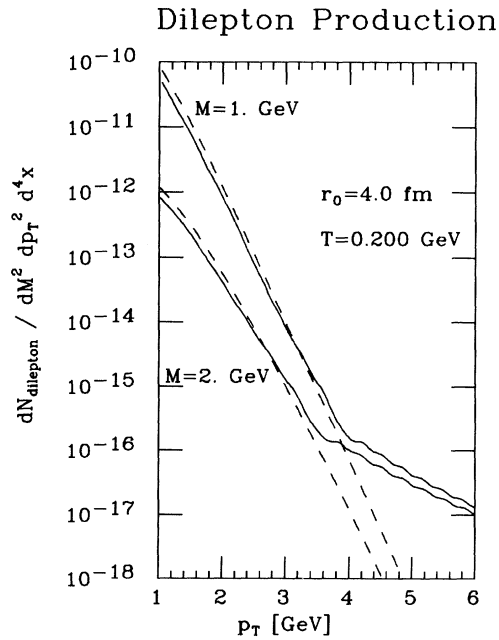

FIG. 2. Dilepton production probability $dN_{l^+l^-}/dM^2dP_T^2d^4x$ for $T = 200$ MeV, $r_0 = 4$ fm, and $P_z = 0$ as a function of the transverse momentum P_T of the dilepton pair. The solid curves are for the case with the boundary, and the dashed curves are the predictions from the Fermi-Dirac distribution.

and $w(\epsilon)$ is

$$w(\epsilon) = -\left\{ \frac{d^2}{dE^2} \left[\ln f(E) + \ln F\left(\frac{M^2}{4E}\right) \right] \right\}_{E=\epsilon}. \quad (14)$$

For a distribution $f(E)$ that is locally an exponential near $E = M/2$, we find $\epsilon \sim M/2$, and the production probability for a given dilepton transverse mass M_T is proportional to $[f(M_T/2)]^2$. Using Eq. (12) [11] and the local-exponential approximation, we show in Fig. 2 the differential probability $dN_{l^+l^-}/dM^2 dP_T^2 d^4x$ as a function of P_T for a dilepton pair with a longitudinal momentum $P_z = 0$, plasma radius $r_0 = 4$ fm, and $M = 1$ and 2 GeV. The solid curves are the results for the case with a boundary, and the dashed curves are the predictions from the Fermi-Dirac distribution. As one observes, the production probability for the case with a boundary are orders of magnitude greater than the prediction from the Fermi-Dirac distribution for $P_T > 4.5$ GeV. The deviation increases with the transverse momentum of the dilepton pair.

The presence of an enhanced distribution at very low and very high transverse momenta, in the quark distribution of a system with a boundary, may lead to peculiar features of the transverse momentum distribution of the pion distribution. In this respect, it is of interest to study whether the boundary effects of the quark-gluon plasma may be the origin of the low-transverse-momentum enhancement observed in NA34 [12] and NA35 [13] experiments or the high-transverse-momentum component of produced pions in many JACEE events [14].

Here, we have introduced the idea of the boundary effects for quarks in a plasma. Similar boundary effects are present in the gluon momentum distribution for gluons in the plasma. The quantitative estimates can be refined by using a smooth boundary instead of a sharp boundary. A smooth boundary may lessen the magnitude of the high-momentum tail, but there remains a general tendency for a greater high-momentum tail relative to the Fermi-Dirac distribution.

The author would like to thank Dr. G. Gatoff and Dr. J. Kapusta for helpful discussions. This research was supported in part by the Division of Nuclear Physics, U.S. Department of Energy under Contract No. DE-AC05-84OR21400 managed by Martin Marietta Energy Systems, Inc.

[1] For a review of current research in the area of quark-gluon plasma, see the Proceedings of Quark Matter '91 Meeting, Gatlinburg, 1991, in Nucl. Phys. **A544** (1991).
[2] R. C. Hwa and K. Kajantie, Phys. Rev. D **32**, 1109 (1985).
[3] K. Kajantie, J. Kapusta, L. McLerran, and A. Mekjian, Phys. Rev. D **34**, 2746 (1986).
[4] P. V. Ruuskanen, Nucl. Phys. **A522**, 255c (1991).
[5] H.-T. Elze and W. Greiner, Phys. Lett. **179**, 385 (1986).
[6] H. P. Pavel and D. M. Brink, Z. Phys. C **51**, 119 (1991).
[7] Th. Schönfeld, A. Schäfer, B. Müller, K. Sailer, J. Reinhardt, and W. Greiner, Phys. Lett. B **247**, 5 (1990).
[8] K. Sailer, Th. Schönfeld, A. Schäfer, B. Müller, and W. Greiner, Phys. Lett. B **240**, 381 (1990).
[9] G. Gatoff and C. Y. Wong, Phys. Rev. D **46**, 997 (1992).
[10] *Handbook of Mathematical Functions*, edited by M. Abramowitz and I. A. Stegun (Dover, New York, 1972).
[11] Strictly speaking, Eq. (12) is for a general spherical distribution $f(E)$. For the case where the longitudinal dimension is much greater than the transverse dimension, the longitudinal momentum distribution would be essentially the thermal distribution without the enhanced high-momentum tail. The use of Eq. (12) can still give a good estimate for cases when P_T is large and $P_z \sim 0$.
[12] J. Shukraft *et al.*, Nucl. Phys. **A498**, 79c (1989); B. Jach *et al.*, *ibid.* **A525**, 77c (1991).
[13] B. Renfordt *et al.*, Nucl. Phys. **A498**, 385c (1989).
[14] Y. Takahashi *et al.*, JACEE Collaboration, Nucl. Phys. **A461**, 263c (1987); T. H. Burnett *et al.*, in *Intersections Between Particle and Nuclear Physics (Steamboat Springs, Colorado)*, Proceedings of the Conference on the Intersections of Particle and Nuclear Physics, edited by Richard E. Mische, AIP Conf. Proc. No. 123 (AIP, New York, 1984), p. 723.